Nanoscale

Accepted Manuscript

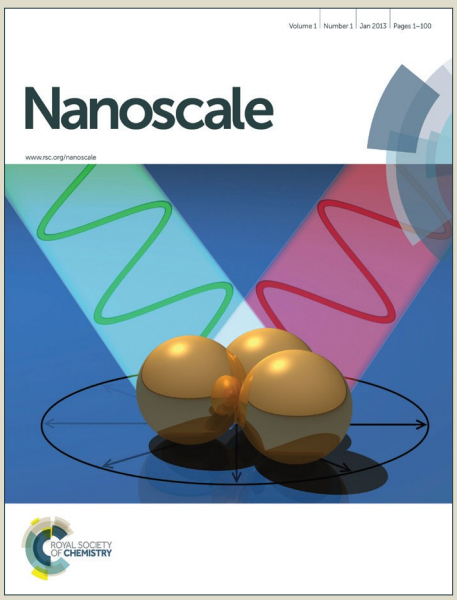

ROYAL SOCIETY OF CHEMISTRY

www.rsc.org/nanoscale

Journal Name

ARTICLE

Responsive polymer brushes for controlled nanoparticle exposure

Namik Akkilic,[a] Frans A.M. Leermakers,[b] and Wiebe M. de Vos[a*]

Received 00th January 20xx,
Accepted 00th January 20xx

DOI: 10.1039/x0xx00000x

www.rsc.org/

We propose the design of a novel mixed polymer brush system that could act as a selective sensor with a distinct on-off switch. In the proposed system, a (single) nanoparticle (such as an antibody) is end-attached to a responsive chain, which is surrounded by a brush of nonresponsive chains. The collapse of the responsive chain leads to a protected state, where the nanoparticle is hidden in the polymer brush, while swelling of the responsive chain brings the nanoparticle outside of the brush into an exposed and active state. We investigate this system by numerical self-consistent field theory and predict a first-order like transition between the active state and the protective state at a critical decrease in solvent quality for the responsive chain. We show that by careful design of the brush parameters such as grafting density and chain length, for a given particle size, it is possible to fine-tune the desired switching mechanism.

Introduction

An assembly of polymer chains that are tethered to an interface by one or more anchoring groups with a grafting density such that the chains interact laterally and therefore stretch in the normal direction is known as a polymer brush.[1] Polymer brushes are among the most powerful systems to create smart surface coatings. We can apply cooperative polymer properties to create polymer brushes, which respond dramatically to external triggers (*e.g.* pH, temperature, ionic strength, solvent quality or an applied potential) which are superior over traditional surfaces. Such a brush may be used to modify the wettability of a surface,[2-5] control the cell and bacterial adhesion[6-12] and tune protein adsorption.[6, 8, 11, 13-15] In nanobiotechnology and material science we see many applications emerge wherein polymer brushes are combined with or interact with nanoparticles (NP), *e.g.* proteins, enzymes, inorganic NP's.[16-19] In combination with responsive polymer brushes, such functional coatings become even more promising for regenerative medicine,[20] protein carriers[21] and (bio)sensors.[20, 22-27]

Compared to the ingenious mechanism found in nature wherein macromolecules (proteins, DNA), fine-tuned by evolution, feature in specific and complex tasks, man-made applications are rough and primitive. One way to bridge the gap with biology is to combine a brush with biological active species such as enzymes, antibodies or receptors. When this is implemented in such a way that the responsive nature of its polymeric ingredients is exploited, we arrive at an interesting advanced type of surface coatings.

In this work, we propose a mixed polymer brush system that by combination of two chemically different polymer chains in one brush brings in new opportunities to control surface properties (Fig. 1). In this mixed brush, we consider a nanoparticle that is end-attached to an minority, active chain surrounded by unresponsive chains. This responsive polymer brush that with certain trigger switches between a protective state, in which the biological component is hidden deep inside a protective brush layer (black curves represents non-responsive chains), and an active state in which the biological component is exposed to the solution. From Figure 1, it can be clear that an experimental design of such a system is rather complex, as many parameters such as particle size, grafting density and chain length play a critical role.[28-31] To make this design work efficiently, a molecularly-detailed theoretical investigation is paramount. The Scheutjens-Fleer self-consistent field (SF-SCF) method is a numerical approach to model polymers at interfaces and has been successfully applied to polymer brushes.[32] The method compares favourably to Monte Carlo and Molecular Dynamics

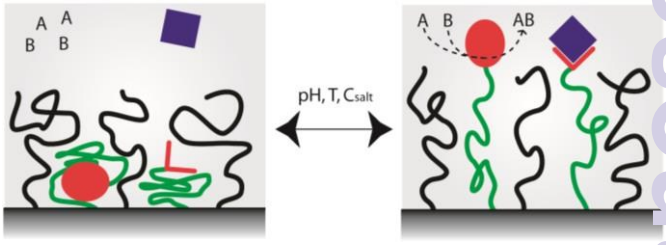

Figure 1. Schematic representation of a biomolecule end-attached to a responsive chain in the mixed polymer brush. Green curves and black curves are the minority responsive chains and non-responsive chains, respectively. A change in pH, temperature or salt concentration leads to a conformational change in the active chain

[a] *Membrane Science and Technology, Mesa+ Institute for Nanotechnology, University of Twente, P.O. Box 217, 7500 AE Enschede, The Netherlands.*
[b] *Laboratory of Physical Chemistry and Soft Matter, Wageningen University, Dreijenplein 6, 6703 HB Wageningen, The Netherlands.*
[*] *Corresponding Author: w.m.devos@utwente.nl*

†Electronic Supplementary Information (ESI) available: Brush density profiles for different grafting densities and chain lengths and probability distributions of nanoparticles with different sizes. See DOI: 10.1039/x0xx00000x

simulations, but is computationally many orders of magnitude more efficient. One of the pioneering work[33] on brush-particle interactions by SF-SCF calculated the free energy of the brush for a particle penetrating a brush at different grafting densities, particle sizes and distances from the grafting interface. Following this investigation, Chen and Ma [34] showed an effective interaction between two colloidal particles when they penetrated in polymer brush at the different depths and particles sizes. Moreover, effective brush-mediated interaction between nanoparticles depends strongly on the shape of the nanoparticles, where vertically aligned particles attract each other and the particles at the same horizontal level repel.[35]

We employ SF-SCF theory to demonstrate the feasibility of the complex system proposed in Figure 1, while at the same time elucidating the key parameters. Our calculations on free energy profiles precisely show the position of a single-nanoparticle that is specifically attached to the end-group of a polymer chain, depending on the interaction parameter (χ). Using the SF-SCF theory simulations, we are able to predict the location of a nanoparticle, which is attached to a minority responsive polymer chain, inside a brush of unresponsive polymers. We will demonstrate that a jumplike switching is expected between an on- and off-state at the exact trigger (e.g. temperature, pH, salt concentration) at which the switch take place can be fine-tuned by the brush design (e.g. polymer chain length, and the brush density) and size of the particle.

Model and methodology

To accurately model polymer brushes, it is necessary to solve the Edwards (diffusion) equation for polymer chains in inhomogeneous systems:[36]

$$\frac{\partial G(\mathbf{r},s\,|1,1)}{\partial s}=\left(\frac{1}{6}\nabla^2-u(\mathbf{r})\right)G(\mathbf{r},s\,|1,1) \qquad [1]$$

where the Green's function *G* represents the statistical weight of all possible conformations of polymer chains with segment *s'* = 1 next to the surface (r_z = 1) and segment *s'* = s at coordinate r. This quantity is closely related to the chain partition function (that is, when *s* = *N*) and hence to the free energy of the system. In equation (1), it is necessary to specify the (dimensionless) segment potential *u*(r). The role of the segment potential is to mimic the excluded-volume interactions as this result from, e.g., molecular crowding effects. This potential also accounts for the solvent quality. Here and below we assume that the solvent quality is good for the non-responsive polymers: the Flory-Huggins parameter $\chi = 0$. In this case the bare second virial coefficient $v = 1 - 2\chi$ is unity.[37] Assuming for a moment that there is only one relevant coordinate, namely the distance to the wall (for which we use the *z*-coordinate), the segment potential becomes self- consistent when $u(z) = v\varphi(z)$. A polymer chain should connect its free end, irrespectively to the *z*-position of this (free) end, to the grafting segment by taking *N* steps in this potential field. The system can realize this by insisting on a parabolic shape of the segment potential, that is $u(z) = A - Bz^2$. A parabolic potential directly leads to the well-known parabolic volume fraction profile for a dense brush where the chains are strongly stretched.[37, 39]

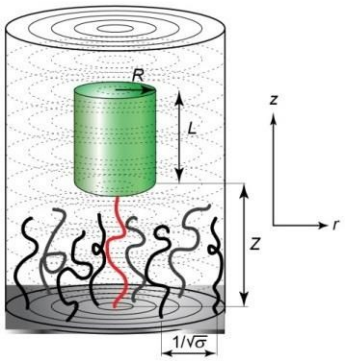

Figure 2. Schematic representation of the coordinate system used in the SF-SCF calculations. Here we show a small particle (top green cylinder) with radius *R* and height *L* positioned at a distance *Z* from the substrate. The particle is attached to a single minority responsive chain (red curve) placed in the middle of a brush of non-responsive chains (black curves). The two-gradient coordinate system (*z*,*r*) is indicated: layers parallel to the surface are numbered *z* = 1, 2, ...,M_z. In radial directions the lattice shells are numbered *r* = 1, 2, ...,M_r. At the surface, a polymer brush with grafting density σ and chain length *N* is present. In the SCF model, we assume that the brush chains are laterally mobile along the surface. To avoid adverse effects of the finite size of the computation box, the boundary condition in the radial direction is mirror-like.

The differential equation (Eq. 1) highlighted above is solved numerically in a two-gradient coordinate system (Fig. 2) to high precision.[40-42] Such a two gradient model is essential to properly model the penetration of brush system by a particle, but also allows a good description of a collapsing polymer chain at decreasing solvent quality. For an obtained solution, we can evaluate the mean-field free energy of the system,

$$F(\{n\},V,T)=-kT\ln Q(\{n\},V,T) \qquad [2]$$

where *Q* is the canonical partition function and *n* is the total number of molecules in the system. Other quantities have their usual meaning. In this system, the characteristic function is a partial open free energy given by:

$$F^{(\mathrm{po})}=F-\sum_i \mu_i n_i \qquad [3]$$

In this equation, μ is the chemical potential and *n* is the number of molecules. The summation runs over all molecules of of which not the number, but the bulk concentration is fixed. We now refer to the z-coordinate of the center of mass of the protein as the distance *Z* of the protein to the surface. Systematic variation of *Z* gives insight in the insertion free energy, which is computed by

$$\Delta F(Z)=F^{(\mathrm{po})}(Z)-F^{(\mathrm{po})}(\infty) \qquad [4]$$

where the latter term is calculated for the case that the protein-like inclusion is far from the brush without stretching

the minority responsive chain (attached to the particle) too much, that is for $Z \rightarrow 50$. One of our interests is in how the preferred location of the attached particle changes when we lower the solvent quality of the minority responsive chain.

The Scheutjens-Fleer Self-Consistent-Field Approach and Parameter Setting

All theoretical details of the equations outlined above and in particular, how these have been implemented in the lattice model of Scheutjens and Fleer are readily available in the literature.[32, 40, 43] Hence, we will not repeat this here.

The coordinate system is an important ingredient that is taken by the method as an input. It specifies exactly how the local mean field approximation is implemented, and this has direct consequences for the type of inhomogeneities that can develop. The current problem calls for a two-gradient coordinate system which is schematically shown in Figure 2. More specifically, we use a cylindrical coordinate system with rotational symmetry. Gradients in segment concentration may develop both in a radial direction, for which we use the r-coordinate, and in the direction along the cylinder axis, that is the z-direction. The solid phase (substrate) is positioned at negative z-values; the surface is at z = 0, and the first layer accessible for molecules is z = 1. The latter layer is where the first segments of the polymer chains are confined to. In principle, there are two options for grafting these chains. One can either restrict the lateral mobility or allow for it. We have chosen for the latter. The lattice layers parallel to the surface are split up in concentric rings of lattice sites over which the meanfield approximation is applied. This means that we ignore the density gradients in these rings. The system size in the radial direction is set by M_r = 20, which is sufficient to allow the perturbations caused by the protein inclusion to relax. The system in the z-direction extends to M_z = 100. At this layer mirror-like boundary conditions are implemented.

The overall grafting densities used in this work are σ = 0.05, σ = 0.1 and σ = 0.2 that are in the range of common experimental values (σ = 0.01-0.3 polymer chains/nm^2).[29, 44] To describe the particle size, we use an object with a radius of R and a height of L lattice sites (LS). We refer to these numbers as (R × L). In this work we have compared three different particles sizes with 1×3; 3×3; 5×3. The volume of our cylindrical particles is thus simply equal to LπR^2 lattice sites. Here 3 x 3 and 5 x 3 were chosen to reflect the size of proteins and/or small inorganic nanoparticles (taking one lattice site to be 1 nm), while 1 x 3 reflects a smaller molecule. The interaction between the particle and polymer segments in the brush is kept constant ($\chi_P = 0$), and the interaction of the polymer segments with the solvent is given by χ. Further interaction parameters, such as the interaction between the minority and majority polymer chains, the interaction between the solvent and the majority polymers and any interactions with the surface are also kept constant at a value of 0. In this way, we really focus on the responsive behavior of the minority chain attached to the nanoparticle.

Results and Discussion

Free energy profile

The Scheutjens-Fleer self-consistent field method generates for the macromolecules in the system the statistical weight for all possible and allowed freely-jointed chain conformations on a lattice. When the first segment of the chain is constrained to be attached to the surface, we obtain the segment density (volume fraction) profiles. Typically, the brush is submerged in a monomeric solvent. The solvent quality is parametrised by the Flory-Huggins interaction parameter χ. The number of segment-solvent interactions is estimated using the Bragg-Williams mean field approximation. The optimal structure of the brush is found after the optimization of the mean field free energy under the constraint that the sum of the polymer and solvent densities is unity (incompressibility relation).

Herewith, we first focus on the mixed brush system proposed in Figure 1, as modeled in Figure S1. A single responsive minority chain (N = 100) is surrounded by a brush of unresponsive chains (σ = 0.1, N = 100). The minority chain is connected to the grafting interface on one side, and to a particle with dimensions 3×3 on the other side. To predict the preferential location of the nanoparticle, we have calculated the change in free energy when this single particle is moved from outside of the brush (Z = 50) to a distance closer to the grafting interface. The resulting change in free energy (ΔF) profiles is shown in Figure 3 as a function of distance (Z) (where Z = 50 is set at brush zero point ΔF = 0). All energies are given in units of the thermal energy k_BT.

Here, the Flory-Huggins interaction parameter (χ) between the responsive polymer and the solvent can be seen as the "trigger" (e.g. pH, temperature, ionic strength, voltage) that induces collapse of the responsive polymer chain. For poly(*N*-isopropylacrylamide) (PNIPAM) at lower polymer concentrations, a switch between an hydrophilic state (<32°C) and a hydrophobic state (>32°C) is associated with a change in χ from approximately 0.3 to 1.1.[45,46] For a weak polyelectrolyte such as poly(2-dimethyl aminoethyl methacrylate) (PDMAEMA), much lower χ values (>2) can be obtained in the uncharged state by copolymerization with the hydrophobic butyl methacrylate (BMA), while retaining strong swelling properties at a pH where PDMAEMA becomes charged.[47] Clearly, a wide range of χ values is experimentally achievable with responsive polymers.

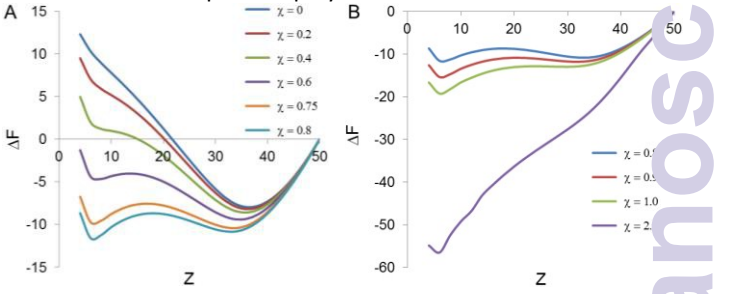

Figure 3. Free energy of interaction (ΔF) between a nanoparticle with a particle size 3×3 and polymer brush with a chain length N = 100 and grafting density σ = 0.1 as a function of distance (Z) from the grafting interface. A) $0 \leq \chi \leq 0.7$ and B) $0.8 \leq \chi \leq 2$

When there is no attractive interaction between the segments of the polymer, at $\chi = 0$ (Fig. 3A), ΔF shows a minimum value when the particle is located just at the edge of the brush (Z = 36, see also Fig. 4A) as the polymer density in the brush decreases rapidly between Z=30 and Z=50 (Fig. S1) for σ = 0.1, N = 100. At this position, the particle has hardly any excluded volume interactions with the polymers in the brush, while the responsive minority chain is stretched to the same extend as the other polymers in the brush. Moving the particle into the brush (Z < 36) is unfavorable because of excluded volume interactions, moving the particle away from the brush (Z > 36) is unfavorable, as it would lead to stretching of the minority chain. However, this balance of forces shifts when we decrease the solvent quality for the responsive chain (by increasing χ). A collapse of the responsive polymer becomes favorable, as observed from a second minimum in the free energy, but this does mean that the particle needs to enter the brush. Between χ is 0.7 and 0.8 the collapse of the responsive polymer chain becomes so favorable that it is able to overcome the excluded volume interactions between brush and particle and the lowest minimum in the free energy becomes the one where the particle is located deep within the brush Z = 6. Two co-existing minima in the free energy that move past each other are a clear indication of a (quasi) first order phase transition. Above χ = 0.9, the minimum in the free energy close to the interface become very dominating (Figs. 3B and 4B). These findings are very encouraging as they demonstrate that under reasonable conditions a nanoparticle can be moved in and out of a brush by changing the solvent quality of a responsive chain connected to the nanoparticle. Because the barrier between the minima is not infinitely high, the transition is (quasi) first order and therefore thermal fluctuations allow the chains to switch from the brush interface to the deep with the polymer brush.

Probability of a particle being inside a brush

To show the transition of the particle location more clearly, we have calculated the probability distributions from the free energy profiles (Fig. 3) as shown in Figure 4A (see also Fig. S2 for different particle sizes). When there is no or minimum interaction between the brush and particle (χ = 0-0.6), the total number of degrees of freedom becomes large enough, and thus the canonical probability distribution peaks around the position Z = 36. This canonical probability distribution can thus be well approximated by a Gaussian distribution centered at the outside of the brush. Further increasing the interaction parameter from χ = 0.6 to 0.9 leads to a binodal distribution where the particle is either located at the edge of the brush or deep inside of the brush. At χ > 0.9, binodal distribution disappears and probability distribution peaks sharply around the position Z = 6 as seen in Figure 4A. In Figure 4B, we show the systematic investigation of the relation between the most probable distance, Z, and the average distance, <Z>, of a nanoparticle from the grafting interface as a function of interaction parameter, χ. The most probable distance of the

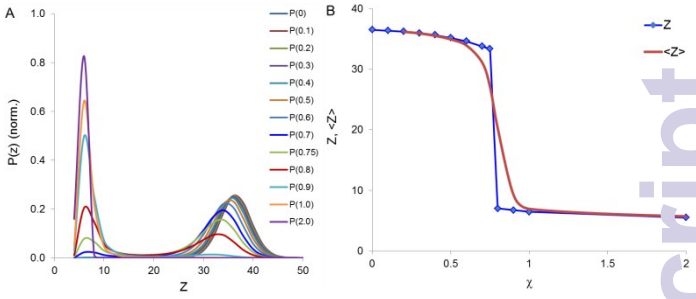

Figure 4. (A) Probability distributions of a nanoparticle end-attached to a polymer brush as a function of distance from the grafting interface for various interaction parameters: from χ = 0 to = 3.0 ; Particle size is 3×3, σ = 0.1. (B) Distance (Z) and average distance (<Z>) of a nanoparticle end-attached to a polymer brush from the grafting interface as a function of Flory-Huggins interaction parameter (χ). N = 100, σ = 0.1 and particle size 3×3.

nanoparticle with a size of 3×3 to the grafting interface (N = 100, σ = 0.1) was obtained by simply taking the lowest point in the free energy profiles (Fig. 3). Figure 4B shows more clearly, what was discussed before. There are two optimal positions for the nanoparticle, either at the edge of the brush or deep inside of the brush. Between χ = 0.7 to χ = 0.9 there is a smooth but sharp transition from one state to the other.

Effect of particle size and grafting density

The difficulty for a particle to penetrate a polymer brush is governed by two key parameters: The polymer density in the brush (connected to the grafting density) and the size of the particle. To investigate in detail how these two parameters will influence the switching of a particle in and out of the brush, we have considered three different particle sizes with 1×3, 3×3 and 5×3 (L x R) and three different grafting densities 0.05, 0.1 and 0.2. For all these conditions (Fig. 5) we see generally the same behavior, there are two optimal positions for the particle, one at the edge of the brush (the location of which depends on the grafting density, see Fig. S1A) and one deep inside of the brush. By changing the solvent quality of the minority chain there is a switch from one position to another. What is determined by the combination of grafting density and particle size is the χ value at which the transition takes place and the sharpness of the transition. For a small particle (1×3) and low grafting density (Fig. 5A), the particle can easily penetrate the brush as also seen in the probability distributions (Fig. S2A), and thus a low decrease of solvent quality for the responsive polymer (~0.3) is sufficient to pull the particle into the brush. For these conditions, the transition is also quite gradual in nature. However, for higher grafting densities the transition becomes sharper and moves to higher values of χ. Increasing particle size also leads to transitions at higher χ value and to sharper transitions (Figs. 5B and 5C, see the probability distributions in Figs. S2B-C).

These results show very clearly that the switch from an exposed particle to a protected particle is the result of a force balance. On one hand, there is the force as a result of excluded volume interactions that pushed the particle to the edge of the polymer brush. On the other hand, a decrease of solvent

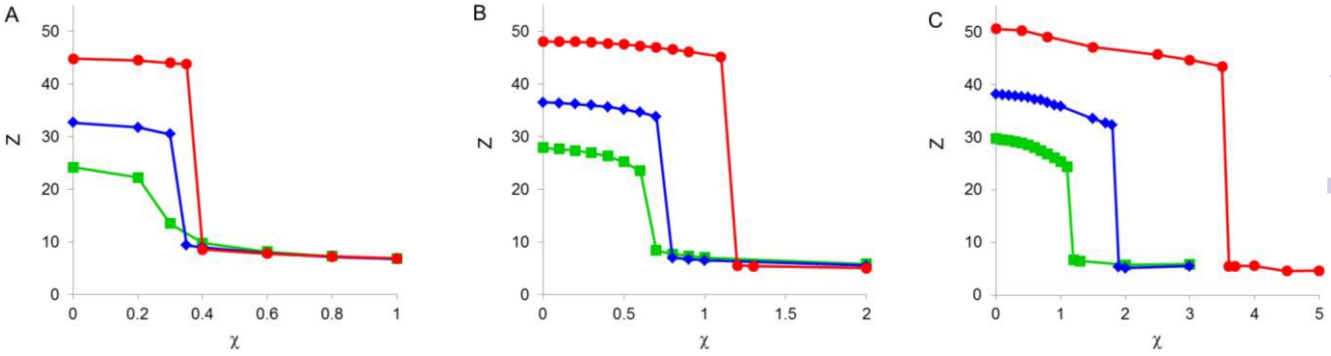

Figure 5. Position of a nanoparticle from the grafting interface as a function of Flory-Huggins interaction parameter (χ) at grafting densities of σ = 0.05 (green), σ = 0.1 (blue) and σ = 0.2 (red). N = 100. A) 1×3; B) 3×3; C) 5×3.

quality for the responsive polymer chain leads to a force on the particle pulling it inside of the brush. A switch in location occurs when the pulling force becomes larger than the pushing force or vice versa. These results indicate, that by carefully balancing the grafting density of the brush and the size of the attached bio-macromolecule, one could control the exact pH, salt concentration or temperature (represented here by χ) at which the transition occurs.

Effect of chain length

The other key parameter of any polymer brush is considered to be the chain length. To investigate the chain length effect on the penetration of a nanoparticle, we consider the main polymer chain of the non-responsive chains with chain length (N_1) is fixed while the chain length of responsive minority chains (N_2) are varied (Fig. 6A). We have considered three different responsive chain lengths (N_2): (1) $N_2 < N_1$; (2) $N_2 = N_1$ and (3) $N_2 > N_1$. Here, the size of the nanoparticle which is end-attached to the responsive polymer chain is 3×3 and grafting density is σ = 0.1. In the case of N_2 (50) < N_1 (100), the most probable location for the particle is inside of the brush layer, even at χ = 0. For the short chain, stretching all the way to the edge of the brush is too unfavorable and as such, the particle is already pulled into the brush (Fig. 6B, green curve). A further decrease of solvent quality leads to a gradual change to a position close to the interface. As the particle is already in the brush, there is no large excluded volume penalty to p... the responsive polymer chain to collapse, and as a result, th... transition is very gradual. As discussed before, when the lengths are equal (N_2 = N_1 = 100) for both chains, a sharp transition from outside of the brush (Z = 36) and to deep inside (Z = 6) was predicted (Fig. 6B, blue curve). If the responsive chain length is larger than that of the unresponsive brush chains, N_2 (200) > N_1 (100), we observed a slow transition from just above the edge of the brush to the edge of the brush (r... curve in Fig. 6). This is similar to what is observed for minority chain behavior in a polymeric brush.[48-50] Under these conditions, much of the long polymer can already form a dense coil (collapse) without the particle having to penetrate the brush. Only at very poor solvent qualities, we find the transition of the particle from the edge of the brush to inside of the brush. From these results, we can conclude that in general it will be favorable to have both the responsive and the unresponsive chains of approximately the same chain length as this provides the sharpest switching at m... reasonable values of χ.

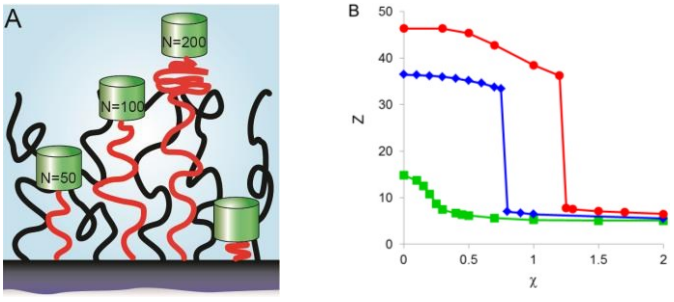

Figure 6. (A) Illustration of nanoparticle position from the grafting interface as a function of active chain length (N_2). Particle (green) is attached to the end-group of an active chain (red curves). Nonresponsive chain (black curves) length N_1 = 100, grafting density σ = 0.1 and particle size 3×3 are constants. (B) Position of a nanoparticle from the grafting interface as a function of Flory-Huggins interaction parameter (χ) at different active chain lengths: N_2 = 50 (green); N_2 = 100 (blue) and N_2 = 200 (red).

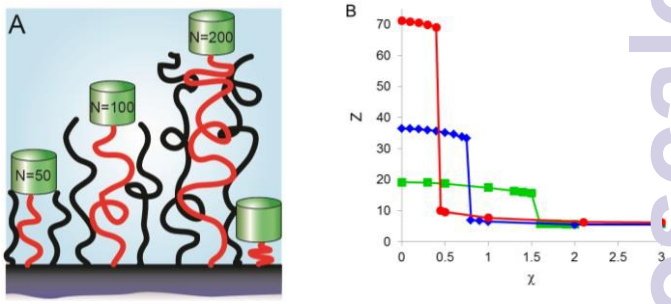

Figure 7. (A) Illustration of nanoparticle position from the grafting interface as a function of active chain length (N_2). Particle (green) is attached to the end-group of a... active chain (red curves). Active chain length kept equal to the nonresponsive chai... length at each condition. Particle size is 3×3. (B) Position of a nanoparticle from t... grafting interface as a function of Flory-Huggins interaction parameter (χ) at different active chain lengths: N_1 = 50 and N_2 = 50 (green); N_1 = 100 and N_2 = 100 (blue) and N_1 = 200 and N_2 = 200 (red).

We can further design a mixed brush system, considering the responsive chain length equal to the nonresponsive chains. In Figure 7, we have illustrated such a system with chain length equal to 50, 100 and 200 for both types of chains. Again, the size of the nanoparticle which is end attached to the responsive polymer chain is 3×3. For all chain lengths, we find sharp switching between two optimal locations, at the edge of the brush (which varies with *N* as shown in Fig. S1B) and deep inside of the brush. However, the critical χ parameter at which the transition between the two locations occurs is strongly influenced. For the longest chain length the critical χ is around 0.45, while for the shortest (N = 50) critical χ is as high as 1.6. This is opposite to what was observed in Figure 6, when only the chain length of the responsive chain was varied. This can be explained by a simple energy balance: A longer chain length of the whole brush has no effect on the energy required to pull a particle into the brush as the brush density remain the same. However, a longer chain gains much more energy from collapsing with a larger number of monomers clustering together. Furthermore, a larger collapsed coil has better volume to surface ratio, meaning that a lower fraction of monomers will interact with the (poor) solvent.

In the proposed mixed polymer brush system (Fig. 1), a conformational change for the active chain (green curves) can be triggered by varying parameters such as temperature (*e.g.* PNIPAM), pH and/or ionic strength (*e.g.* poly(methacrylic acid)) while the other polymer chains (black curves) are mainly non-responsive (*e.g.* poly(ethylene oxide)). A biomolecule, for example, an enzyme is then tagged to the end-group of the responsive chain as shown in Figure 1 (red sphere). This enzyme will bind to its substrate to form the product only when it is exposed to the bulk solution by an external trigger. Accordingly, glucose oxidase was covalently attached to a poly(glycidyl methacrylate) and poly(2-hydroxyethylmethacrylate) mixed brush to generate a glucose sensor.[27] Another approach can be use of an antibody and/or receptor molecule (red V-shape) end-attached to responsive chain.[20, 51] Consequently, this receptor molecule will capture a specific target molecule when it is exposed to the surface. Simultaneously, non-specific adsorption of target molecules either to the surface or receptor molecule are prevented by the non-responsive, second brush (black curves) such as poly(ethylene oxide).[6, 10, 20] By preventing the adsorption of protein molecules and bacteria, the brush helps to prevent the growth of microorganisms, so-called biofilm[9, 52] and thus possible infections. As investigated experimentally, grafting density and chain length are the two key parameters to control the interfacial properties of a polymer brush.[12, 28-31, 53] By varying the interaction parameter, χ, by means of controlling the pH (or salt concentration),[11, 28, 54-56] temperature[5, 28, 44] or voltage[23] it is indeed possible to obtain a sharp transition of a responsive (homo)polymer brush from a stretched state to collapsing state. Similar to our results shown in Figure 6, Dori and coworkers[53] showed that accessibility of a peptide ligand on a surface to cells can be controlled by varying the non-responsive PEG lipid lengths.

Conclusions

In this manuscript, we propose the design of a novel mixed polymer brush that could act as a very selective biosensor with a clear on-off switch. In the proposed mixed polymer brush system, a nanoparticle (such as an antibody or a catalytic nanoparticle) is end-attached to responsive chain surrounded by a brush of nonresponsive chains. Collapse of the responsive chain leads to a protected state, where the nanoparticle is hidden in the polymer brush, while swelling of the responsive chain brings the nanoparticle outside of the brush into an exposed and active state. By use of SF-SCF theory, we investigated this system theoretically to establish if the proposed system is feasible, and what the critical design parameters are. For given grafting density, chain length and solvent quality (for the responsive chain), the free energy was calculated for all possible particle positions. For a good solvent for the responsive chain, the nanoparticle is always located at the edge of the polymer brush. In this way the responsive chain has the optimal stretching (identical the other polymer chains) while the nanoparticle is still outside of the brush. A decrease in solvent quality however, at a critical χ value, leads to a sharp (quasi first order) transition where the nanoparticle moves to a position deep inside of the brush. The grafting density, particle size and chain length together determine this critical χ value, with larger grafting density and particle size leading to an increase (a larger penalty for particle penetration) while a longer chain length leads to decrease (more energy gain upon chain collapse). The most optimal switching is found when the responsive chain and the surrounding non-responsive brush have approximately the same chain length. Our theoretical results confirm the large potential of our proposed system. Switching of the nanoparticle occurs between a well-defined exposed and a protected state and is expected to show a sharp transition at a well-defined solvent quality for the responsive chain. The exact solvent quality can be tuned/optimized by (for a given nanoparticle size) tuning the grafting density and chain length. We believe these findings can be used to experimentally develop this polymer/nanoparticle system for responsive fast and specific (bio)sensors at the single-molecule sensitivity. Experimental design for such a system is underway.

Acknowledgements

WdV acknowledges financial support from the Netherlands Organisation for Scientific Research (NWO) under programme VENI 722.012.008.

References

1. T. P. Russell, *Science*, 2002, **297**, 964-967.
2. X. Zeng, G. Xu, Y. Gao and Y. An, *The Journal of Physical Chemistry B*, 2010, **115**, 450-454.
3. M. Motornov, S. Minko, K.-J. Eichhorn, M. Nitschke, F. Simon and M. Stamm, *Langmuir*, 2003, **19**, 8077-8085.

4. J. Elbert, M. Gallei, C. Rüttiger, A. Brunsen, H. Didzoleit, B. Stühn and M. Rehahn, *Organometallics*, 2013, **32**, 5873-5878.
5. O. Azzaroni, A. A. Brown and W. T. S. Huck, *Angew. Chem. Int. Ed.*, 2006, **45**, 1770-1774.
6. H. Du, P. Chandaroy and S. W. Hui, *Biochimica et Biophysica Acta (BBA) - Biomembranes*, 1997, **1326**, 236-248.
7. L. Yang, F. Pan, X. Zhao, M. Yaseen, F. Padia, P. Coffey, A. Freund, L. Yang, T. Liu, X. Ma and J. R. Lu, *Langmuir*, 2010, **26**, 17304-17314.
8. Q. Yu, Y. Zhang, H. Chen, F. Zhou, Z. Wu, H. Huang and J. L. Brash, *Langmuir*, 2010, **26**, 8582-8588.
9. A. Gristina, *Science*, 1987, **237**, 1588-1595.
10. A. Roosjen, H. J. Kaper, H. C. van der Mei, W. Norde and H. J. Busscher, *Microbiology*, 2003, **149**, 3239-3246.
11. A. M. Alswieleh, N. Cheng, I. Canton, B. Ustbas, X. Xue, V. Ladmiral, S. Xia, R. E. Ducker, O. El Zubir, M. L. Cartron, C. N. Hunter, G. J. Leggett and S. P. Armes, *Journal of the American Chemical Society*, 2014, **136**, 9404-9413.
12. J. Yang, M. Zhang, H. Chen, Y. Chang, Z. Chen and J. Zheng, *Biomacromolecules*, 2014, **15**, 2982-2991.
13. M. F. Delcroix, G. L. Huet, T. Conard, S. Demoustier-Champagne, F. E. Du Prez, J. Landoulsi and C. C. Dupont-Gillain, *Biomacromolecules*, 2012, **14**, 215-225.
14. O. Hoy, B. Zdyrko, R. Lupitskyy, R. Sheparovych, D. Aulich, J. Wang, E. Bittrich, K.-J. Eichhorn, P. Uhlmann, K. Hinrichs, M. Müller, M. Stamm, S. Minko and I. Luzinov, *Advanced Functional Materials*, 2010, **20**, 2240-2247.
15. W. M. de Vos, P. M. Biesheuvel, A. de Keizer, J. M. Kleijn and M. A. Cohen Stuart, *Langmuir*, 2008, **24**, 6575-6584.
16. M. Motornov, R. Sheparovych, R. Lupitskyy, E. MacWilliams, O. Hoy, I. Luzinov and S. Minko, *Advanced Functional Materials*, 2007, **17**, 2307-2314.
17. E. G. Kelley, J. N. L. Albert, M. O. Sullivan and I. I. I. T. H. Epps, *Chemical Society Reviews*, 2013, **42**, 7057-7071.
18. P. Jain, G. L. Baker and M. L. Bruening, in *Annual Review of Analytical Chemistry*, Annual Reviews, Palo Alto, 2009, vol. 2, pp. 387-408.
19. S. Pennadam, K. Firman, C. Alexander and D. Gorecki, *Journal of Nanobiotechnology*, 2004, **2**, 8.
20. M. Krishnamoorthy, S. Hakobyan, M. Ramstedt and J. E. Gautrot, *Chemical Reviews*, 2014, **114**, 10976-11026.
21. M. S. Shim and Y. J. Kwon, *Advanced Drug Delivery Reviews*, 2012, **64**, 1046-1059.
22. A. R. Ferhan, L. Guo, X. Zhou, P. Chen, S. Hong and D.-H. Kim, *Analytical Chemistry*, 2013, **85**, 4094-4099.
23. M. Welch, A. Rastogi and C. Ober, *Soft Matter*, 2011, **7**, 297-302.
24. S. Gupta, M. Agrawal, P. Uhlmann, F. Simon, U. Oertel and M. Stamm, *Macromolecules*, 2008, **41**, 8152-8158.
25. Y. Chen, P. Gai, J. Xue, J.-R. Zhang and J.-J. Zhu, *Biosensors and Bioelectronics*, 2015, **74**, 142-149.
26. M. Ashaduzzaman, A. Anto Antony, N. Arul Murugan, S. R. Deshpande, A. P. F. Turner and A. Tiwari, *Biosensors and Bioelectronics*, 2015, **73**, 100-107.
27. M. E. Welch, T. Doublet, C. Bernard, G. G. Malliaras and C. K. Ober, *Journal of Polymer Science, Part A: Polymer Chemistry*, 2014, **53**, 372-377.
28. T. Chen, R. Ferris, J. Zhang, R. Ducker and S. Zauscher, *Prog. Polym. Sci.*, 2010, **35**, 94-112.
29. E. P. K. Currie, W. Norde and M. A. Cohen Stuart, *Advances in Colloid and Interface Science*, 2003, **100–102**, 205-265.
30. P. Akkahat, W. Mekboonsonglarp, S. Kiatkamjornwong and V. P. Hoven, *Langmuir*, 2012, **28**, 5302-5311.
31. S. Christau, T. Möller, Z. Yenice, J. Genzer and R. von Klitzing, *Langmuir*, 2014, DOI: 10.1021/la503432x.
32. C. M. Wijmans, J. M. H. M. Scheutjens and E. B. Zhulina, *Macromolecules*, 1992, **25**, 2657-2665.
33. B. M. Steels, J. Koska and C. A. Haynes, *J. Chromatogr., A*, 2000, **743**, 41.
34. K. Chen and Y. Q. Ma, *Journal of Physical Chemistry B*, 2005, **109**, 17617-17622.
35. J. U. Kim and B. O'Shaughnessy, *Macromolecules*, 2005, **39**, 413-425.
36. S. F. Edwards, *Proceedings of the Physical Society*, 1965, **85**, 613.
37. Y. B. Zhulina, V. A. Pryamitsyn and O. V. Borisov, *Polymer Science U.S.S.R.*, 1989, **31**, 205-216.
38. R. Israels, J. M. H. M. Scheutjens and G. J. Fleer, *Macromolecules*, 1993, **26**, 5405-5413.
39. S. T. Milner, T. A. Witten and M. E. Cates, *Macromolecules*, 1988, **21**, 2610-2619.
40. J. M. H. M. Scheutjens and G. J. Fleer, *J Phys Chem-Us*, 1979, **83**, 1619-1635.
41. B. M. Steels, J. Koska and C. A. Haynes, *Journal of Chromatography B: Biomedical Sciences and Applications*, 2000, **743**, 41-56.
42. W. M. de Vos, F. A. M. Leermakers, A. de Keizer, J. M. Kleijn and M. A. Cohen Stuart, *Macromolecules*, 2009, **42**, 5881-5891.
43. E. B. Zhulina and F. A. M. Leermakers, *Biophys. J.*, 2007, **93**, 1421-1430.
44. E. Bittrich, S. Burkert, M. Müller, K.-J. Eichhorn, M. Stamm and P. Uhlmann, *Langmuir : the ACS journal of surfaces and colloids*, 2012, **28**, 3439-3448.
45. F. Afroze, E. Nies and H. Berghmans, *Journal of Molecular Structure*, 2000, **554**, 55-68.
46. S. Mendez, J. G. Curro, J. D. McCoy and G. P. Lopez, *Macromolecules*, 2005, **38**, 174-181.
47. A. Emileh, E. Vasheghani-Farahani and M. Imani, *European Polymer Journal*, 2007, **43**, 1986-1995.
48. A. M. Skvortsov, L. I. Klushin and A. A. Gorbunov, *Macromolecules*, 1997, **30**, 1818-1827.
49. L. I. Klushin, A. M. Skvortsov, A. A. Polotsky, S. Qi and F. Schmid, *Physical Review Letters*, 2014, **113**, 068303.
50. S. Qi, L. I. Klushin, A. M. Skvortsov, A. A. Polotsky and F. Schmid, *Macromolecules*, 2015, **48**, 3775-3787.
51. Y. Liu, Y. Zhang, Y. Zhao and J. Yu, *Colloids and Surfaces B: Biointerfaces*, 2014, **121**, 21-26.
52. J. W. Costerton, P. S. Stewart and E. P. Greenberg, *Science*, 1999, **284**, 1318-1322.
53. Y. Dori, H. Bianco–Peled, S. K. Satija, G. B. Fields, J. B. McCarthy and M. Tirrell, *Journal of Biomedical Materials Research*, 2000, **50**, 75-81.
54. L. A. Fielding, S. Edmondson and S. P. Armes, *Journal of Materials Chemistry*, 2011, **21**, 11773-11780.
55. S. Sanjuan, P. Perrin, N. Pantoustier and Y. Tran, *Langmuir*, 2007, **23**, 5769-5778.
56. J. D. Willott, T. J. Murdoch, B. A. Humphreys, S. Edmondson, G. B. Webber and E. J. Wanless, *Langmuir*, 2014, **30**, 1827-1836.